


RESEARCH

Open Access



# The *Podospora anserina* lytic polysaccharide monooxygenase PaLPMO9H catalyzes oxidative cleavage of diverse plant cell wall matrix glycans

Mathieu Fanuel<sup>1</sup>, Sona Garajova<sup>2</sup>, David Ropartz<sup>1</sup>, Nicholas McGregor<sup>3,4</sup>, Harry Brumer<sup>3,4,5,6</sup>, H el ene Rogniaux<sup>1\*</sup> and Jean-Guy Berrin<sup>2\*</sup> 

## Abstract

**Background:** The enzymatic conversion of plant biomass has been recently revolutionized by the discovery of lytic polysaccharide monooxygenases (LPMO) that catalyze oxidative cleavage of polysaccharides. These powerful enzymes are secreted by a large number of fungal saprotrophs and are important components of commercial enzyme cocktails used for industrial biomass conversion. Among the 33 AA9 LPMOs encoded by the genome of *Podospora anserina*, the PaLPMO9H enzyme catalyzes mixed C1/C4 oxidative cleavage of cellulose and cello-oligosaccharides. Activity of PaLPMO9H on several hemicelluloses has been suggested, but the regioselectivity of the cleavage remained to be determined.

**Results:** In this study, we investigated the activity of PaLPMO9H on mixed-linkage glucans, xyloglucan and glucomannan using tandem mass spectrometry and ion mobility–mass spectrometry. Structural analysis of the released products revealed that PaLPMO9H catalyzes C4 oxidative cleavage of mixed-linkage glucans and mixed C1/C4 oxidative cleavage of glucomannan and xyloglucan. Gem-diols and ketones were produced at the non-reducing end, while aldonic acids were produced at the reducing extremity of the products.

**Conclusion:** The ability of PaLPMO9H to target polysaccharides, differing from cellulose by their linkages, glycosidic composition and/or presence of sidechains, could be advantageous for this coprophilous fungus when catabolizing highly variable polysaccharides and for the development of optimized enzyme cocktails in biorefineries.

**Keywords:** AA9, LPMO, Lignocellulose, Biomass, Polysaccharides, Mass spectrometry, Biorefinery

## Background

The use of plant biomass represents an attractive alternative to fossil-based technologies for the production of high-value chemicals [1]. In nature, filamentous fungi produce lignocellulose-degrading enzymes to acquire carbon from plant biomass. Different types of mechanisms for the deconstruction of plant cell walls have been

described in saprotrophic fungi [2], but the involvement of oxidative enzymes was largely underestimated. The recent discovery of a new class of oxidative enzymes, namely lytic polysaccharide monooxygenases (LPMOs), has dramatically broadened the concept of the enzymatic deconstruction of plant cell wall polysaccharides [3–5]. LPMOs represent key cellulolytic enzymes that act at the surface of fibers where they mediate oxidative cleavage of polysaccharide chains. In industry, addition of LPMOs to cellulolytic cocktails leads to the reduction of the enzyme loading required for efficient saccharification of cellulosic biomass [6, 7].

\*Correspondence: Helene.rogniaux@inra.fr; jean-guy.berrin@univ-amu.fr

<sup>1</sup> Unit e de Recherche Biopolym eres, Interactions, Assemblages, INRA, 44316 Nantes, France

<sup>2</sup> Polytech Marseille, UMR1163 Biodiversit e et Biotechnologie Fongiques, INRA, Aix-Marseille Universit e, Avenue de Luminy, 13288 Marseille, France  
Full list of author information is available at the end of the article

Known LPMOs are grouped into the families AA9, AA10, AA11 and AA13 in the CAZy classification [8]. LPMOs all feature a similar histidine brace coordinating the copper ion responsible for the oxidative cleavage of the substrate [9]. Members of the AA9 family are mainly active on cellulose. The few characterized members from AA11 and AA13 families are active on chitin and starch, respectively [10, 11]. In contrast, the AA10s are mostly found in bacteria and exhibit activity on cellulose or chitin [12]. Beside cellulose, AA9 LPMOs are also known to act on xyloglucan and glucomannan [13] as well as soluble celloextrins [14–16]. Activity on xylan was detected only when xylans were in complex with cellulose chains [17].

Lytic polysaccharide monooxygenases from the AA9 family are exclusively found in fungi with large expansion of genes in white-rot fungi and some ascomycetes. The coprophilous fungus *Podospira anserina* displays an impressive array of CAZymes [18, 19] with 189 glycoside hydrolases and 33 genes encoding AA9 LPMOs (*PaLPMO9*), of which seven have been characterized biochemically [15, 20]. These LPMOs are able to oxidatively cleave cellulose with different regioselectivity. For instance, *PaLPMO9E* was shown to produce exclusively C1-oxidized products, while *PaLPMO9H* was reported to release both C1- and C4-oxidized products from cellulose [15, 20]. In addition, the *PaLPMO9H* displayed relatively broad substrate specificity demonstrated by enzyme activity assays using cellulose and cello-oligosaccharides. Activity of *PaLPMO9H* on different kinds of hemicelluloses was suggested based on hydrogen peroxide assay results. Indeed, the repression of hydrogen peroxide production in the presence of different hemicellulose substrates was significant and concentration-dependent for barley  $\beta$ -glucan, glucomannan, lichenan, and xyloglucan while curdlan, pectin, and xylan had no effect on hydrogen peroxide production [15]. The degradation products and regioselectivity of *PaLPMO9H* acting on these substrates remained undetermined.

In the present work, a comprehensive oligosaccharide structural analysis was performed by tandem mass spectrometry (MS) and ion mobility–mass spectrometry on the released products of *PaLPMO9H* following incubation with four hemicellulosic substrates: lichenan, barley mixed-linkage glucan (MLG), konjac glucomannan (GM) and tamarind xyloglucan (XyG). These polysaccharides are widely represented in the cell walls of different monocotyledonous or dicotyledonous plants, and they exhibit different structural features [21]. Similar to cellulose, all contain some (1  $\rightarrow$  4)-linked  $\beta$ -D-glucose residues. Lichenan and MLG are polymers of  $\beta$ -D-glucosyl residues linked through (1  $\rightarrow$  4) and (1  $\rightarrow$  3) linkages. GM is composed of  $\beta$ -D-glucose and  $\beta$ -D-mannose residues,

linked through (1  $\rightarrow$  4) bonds, while XyG is a branched polysaccharide, with a backbone of (1  $\rightarrow$  4)-linked  $\beta$ -D-glucose residues, most of which are substituted with (1  $\rightarrow$  6)-linked  $\alpha$ -D-xylose sidechains which are sometimes further extended with (1  $\rightarrow$  2)-linked  $\beta$ -D-galactose residues. Our objective was to determine the specificity and selectivity of the *PaLPMO9H* enzyme for these structures, differing from cellulose by their linkages, glycosidic composition and/or the presence of sidechains.

## Methods

### Chemicals, substrates and standards

HPLC-grade methanol (MeOH) was purchased from Carlo-Erba (Peypin, France). Ultrapure Water was obtained from a milli-Q apparatus (Merck Millipore, Saint Quentin en Yvelines, France). All other chemicals were purchased from Sigma-Aldrich.

Polysaccharides including lichenan from Icelandic moss, barley MLG, tamarind XyG, konjac GM and  $\beta$ (1,3)/ $\beta$ (1,4)-oligosaccharides including G4A (Glc- $\beta$ (1,3)-Glc- $\beta$ (1,4)-Glc- $\beta$ (1,4)-Glc), G4B (Glc- $\beta$ (1,4)-Glc- $\beta$ (1,4)-Glc- $\beta$ (1,3)-Glc) and G4C (Glc- $\beta$ (1,4)-Glc- $\beta$ (1,3)-Glc- $\beta$ (1,4)-Glc) were purchased from Megazyme (Bray, Ireland). XXXGXXXG (XGO14) was prepared and analyzed by HPAEC-PAD as described in McGregor et al. [22]. Phosphoric acid cellulose was prepared as described in Bennati-Granier et al. [15].

### Enzyme production

*PaLPMO9H* from *Podospira anserina* (Genbank ID CAP61476) was expressed in *Pichia pastoris*, produced in a bioreactor and purified as described previously [15].

### Cleavage assays

All the cleavage assays (300  $\mu$ L liquid volume) contained 4.4  $\mu$ M of *PaLPMO9H*, 1 mM of ascorbate and 0.05% (w/v) of hemicellulose or 0.2 mM XGO14 in milli-Q water. No buffer was used to avoid the formation of multiple salt adducts during the mass spectrometry analyses causing loss of sensitivity or misinterpretations. The enzyme reactions were performed in 2-mL tubes and incubated in a thermomixer (Eppendorf) at 40  $^{\circ}$ C and 500 rpm. After 24 h of incubation, the enzymatic reaction was stopped by filtration through a 10-kDa cutoff polyether sulfone membrane and the soluble products were analyzed by mass spectrometry.

### Mass spectrometry

Experiments were performed on a Synapt G2Si high-definition mass spectrometer (Waters Corp., Manchester, UK). Two types of mass measurements were performed on the samples. First, a mass profile was collected for a mass range of 350–2000  $m/z$ . Second, ion mobility (IM) was activated to collect ion mobility–mass spectra

separating possible isomers and/or reducing interference from sample impurities. IM was performed in a traveling-wave ion mobility (TWIM) cell. The gas flows were held at 180 mL min<sup>-1</sup> He in the helium cell and at 90 mL min<sup>-1</sup> N<sub>2</sub> in the mobility cell. The IM traveling-wave height was set to 40 V and its wave velocity was set to 450 m s<sup>-1</sup> for positive ionization mode and 550 m s<sup>-1</sup> for negative ionization mode. Ions of interest were fragmented after the gas-phase separation by collision-induced dissociation in the transfer cell of the instrument, with an adjustment of the collision energies such that a significant fragmentation was obtained while keeping an observable proportion of the intact precursor. Samples were diluted tenfold in MeOH/H<sub>2</sub>O (1:1, v/v) and infused at a flow rate of 5 μL min<sup>-1</sup> in the instrument. The instrument was operated in positive or negative polarity and in “sensitivity” mode. Data acquisition was carried out using MassLynx software (V4.1).

## Results and discussion

Different sources of hemicelluloses were incubated with *PaLPMO9H* under ascorbate conditions and their reaction products were characterized by mass spectrometry. Four substrates were considered: lichenan, MLG, XyG and GM. Cellulose was also included in the study as a reference substrate. The activity of *PaLPMO9H* products on cellulose has been described in detail and was shown to generate singly and doubly oxidized products at the C1 and/or C4 positions. This results in the formation of gem-diols/ketones at the newly formed “non-reducing” end or aldonic acids at the newly formed “reducing” end [15].

### *PaLPMO9H* demonstrates broad specificity toward β-(1 → 4)-linked glucans

As shown by the mass spectra in Fig. 1b–e, the incubation of *PaLPMO9H* with the four hemicellulosic substrates produced some oligosaccharides having degrees of polymerization (DPs) ranging from 2 to 12, confirming the depolymerizing activity of the enzyme on all of these structures. The most abundant peaks ranged between DP2 and DP4 for lichenan, MLG, and GM. In the case of XyG, DP6 and DP7 were detected with the highest intensity. In addition, the presence of some species with a mass shift of -2 (ketone or lactone) and +16 (gem-diol or aldonic acid) Da relative to the non-modified oligosaccharide suggested an oxidative cleavage activity, in agreement with the previous observations on cellulose [15]. The profiles of the reaction products were quite similar for all hemicellulosic substrates (Fig. 1, right panel). The non-modified species were always the most intense, regardless of the DP, while the intensity of the -2 Da species was either higher or similar to that of +16 Da

species. The situation was slightly different when *PaLPMO9H* was incubated with cellulose (Fig. 1a). The species at -2 and +16 Da were the most intense ions. One additional species of low intensity was detected with a mass shift of +32 Da (*m/z* 721.20) from the related non-modified DP. This species has been described as a doubly oxidized product, with one gem-diol on the non-reducing end (C4), and another oxidation either at the reducing end or at the non-reducing end [15].

These results unambiguously confirmed that *PaLPMO9H* enzyme exhibits a broad specificity toward hemicelluloses compared to other AA9 LPMOs. Subtle differences were observed with respect to the action on cellulose, among which the apparent absence of double-oxidation. In-depth characterization of the reaction products was further carried out by tandem MS to explore the regioselectivity of the oxidative cleavage.

### *PaLPMO9H* oxidatively cleaves β-(1 → 4)- and β-(1 → 4; 1 → 3)-linked glucosidic substrates

Lichenan and MLG are each composed of a linear chain of β-D-glucosyl residues linked by (1 → 4) and (1 → 3) linkages. The proportion and distribution of these β-(1 → 4) and β-(1 → 3) linkages vary between these two substrates; the average ratio of β-(1 → 3):β-(1 → 4) bonds is roughly 1:3 and 1:2 for MLG and lichenan, respectively. To differentiate possible linkage isomers among the reaction products, ion mobility was used in combination with tandem MS. Ion mobility separates species based on their gas-phase conformation prior to their mass measurement. Figure 2 shows the mobilograms recorded for the non-modified species of DP4 obtained for lichenan, MLG and cellulose. As cellulose is exclusively composed of β-(1 → 4) linkages, its degradation was expected to produce a single DP4 species that could be used as a reference. Figure 2 shows that a major peak at a drift time (dt) of 76 bins was detected for the natriated non-oxidized DP4 ion (*m/z* 689.2) arising from cellulose. In contrast, mobility traces indicated the clear presence of at least two gas-phase isoforms for the DP4 released from lichenan and MLG. One of those (dt = 76 bins) corresponded to a DP4 species containing three consecutive β-(1 → 4) linkages (cellotetraose). The second one (dt = 83 bins) was assumed to contain both β-(1 → 3) and β-(1 → 4) linkages. This interpretation was supported by the comparison with three DP4 commercial standards, all containing one β-(1 → 3) linkage (Additional file 1: Figure S1). The presence of one β-(1 → 3) linkage in the oligosaccharide changes the shape of the gas-phase ions and increases the drift time compared to the structure with three consecutive β-(1 → 4) linkages. Similar profiles of ion mobility were observed for the ions having a mass shift of -2 and +16 Da (*m/z* 687.2 and 705.2, respectively) from the

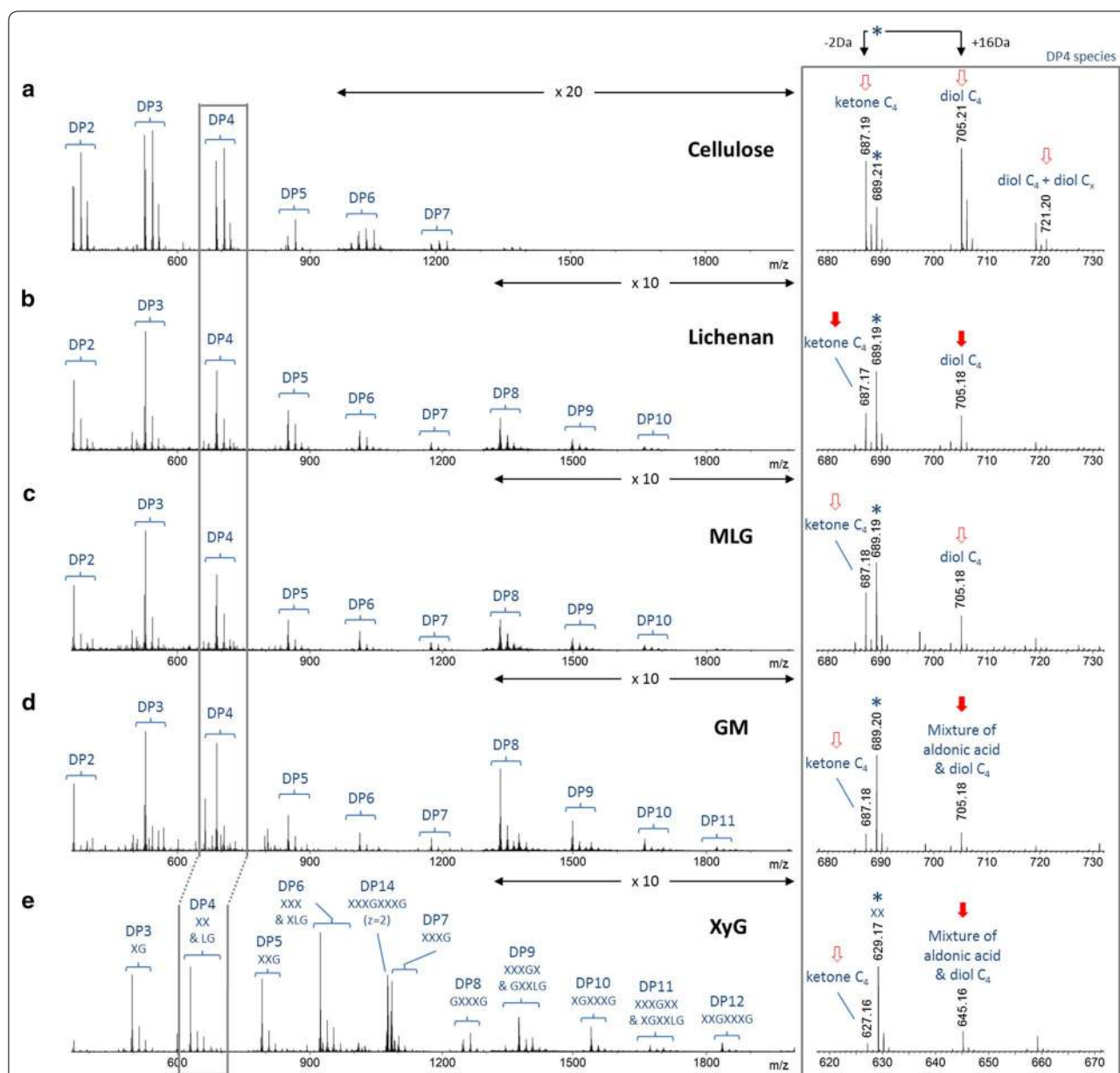
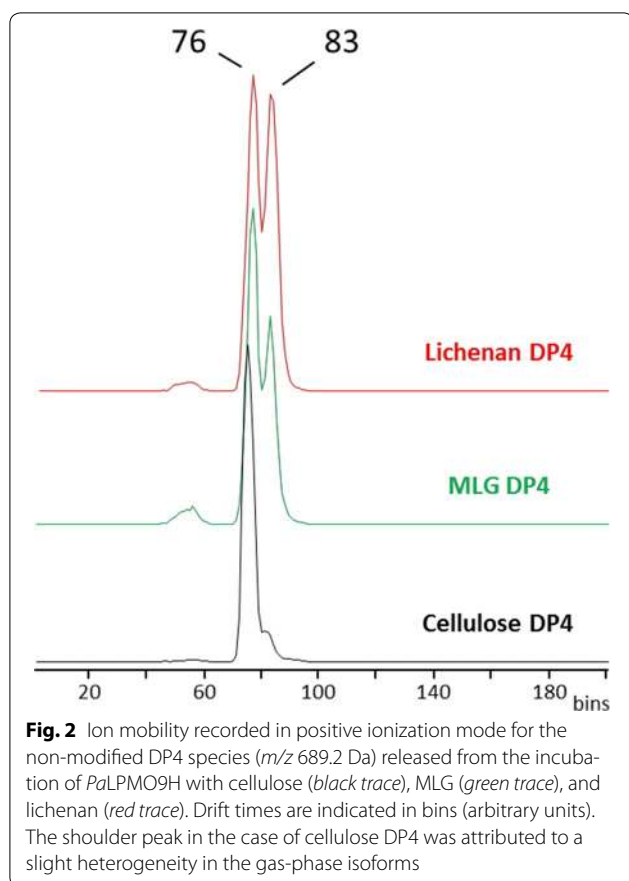


**Fig. 1** ESI-MS spectra showing the degradation products generated from several cellulosic and hemicellulosic substrates by *PaLPMO9H* under ascorbate conditions. **a** Cellulose; **b** lichenan; **c** MLG; **d** GM; **e** XyG. Species were detected as sodium adducts ( $[M+Na]^+$ ) except for XXXGXXXG which was detected as  $[M+2Na]^{2+}$ . The main degrees of polymerization (DP) were annotated. *Right panel* enlarged view of the DP4 species, for all substrates; *stars* the non-modified product. Peaks indicated by an *arrow* were attributed to the oxidized species ( $-2$ ,  $+16$ ,  $+32$  Da relative to the non-modified species) and were further characterized by tandem MS (*full arrow* data presented in the following sections; *empty arrows* data not shown). Labels of the oxidized species were proposed based on tandem MS results. For cellulose: “diol C<sub>4</sub>+ diol C<sub>x</sub>” indicates a double oxidation (diols): one has been localized at C<sub>4</sub> of the non-reducing end, while the second one could not be precisely localized and is either localized at the reducing end or non-reducing end

non-modified DP4, which likely correspond to oxidized products (Additional file 1: Figure S2).

The results thus showed that DP4 species released from lichenan and MLG by *PaLPMO9H* had two main types of structures: one displaying three consecutive  $\beta$ -(1  $\rightarrow$  4)

linkages, the other encompassing at least one  $\beta$ -(1  $\rightarrow$  3) linkage. MLG and lichenan contain a significant proportion of  $\beta$ -(1  $\rightarrow$  3) to (1  $\rightarrow$  4)  $\beta$ -linkages is of 1:3 to 1:2 in these two polymers. In barley MLG, cellodextrin units of two (DP3)



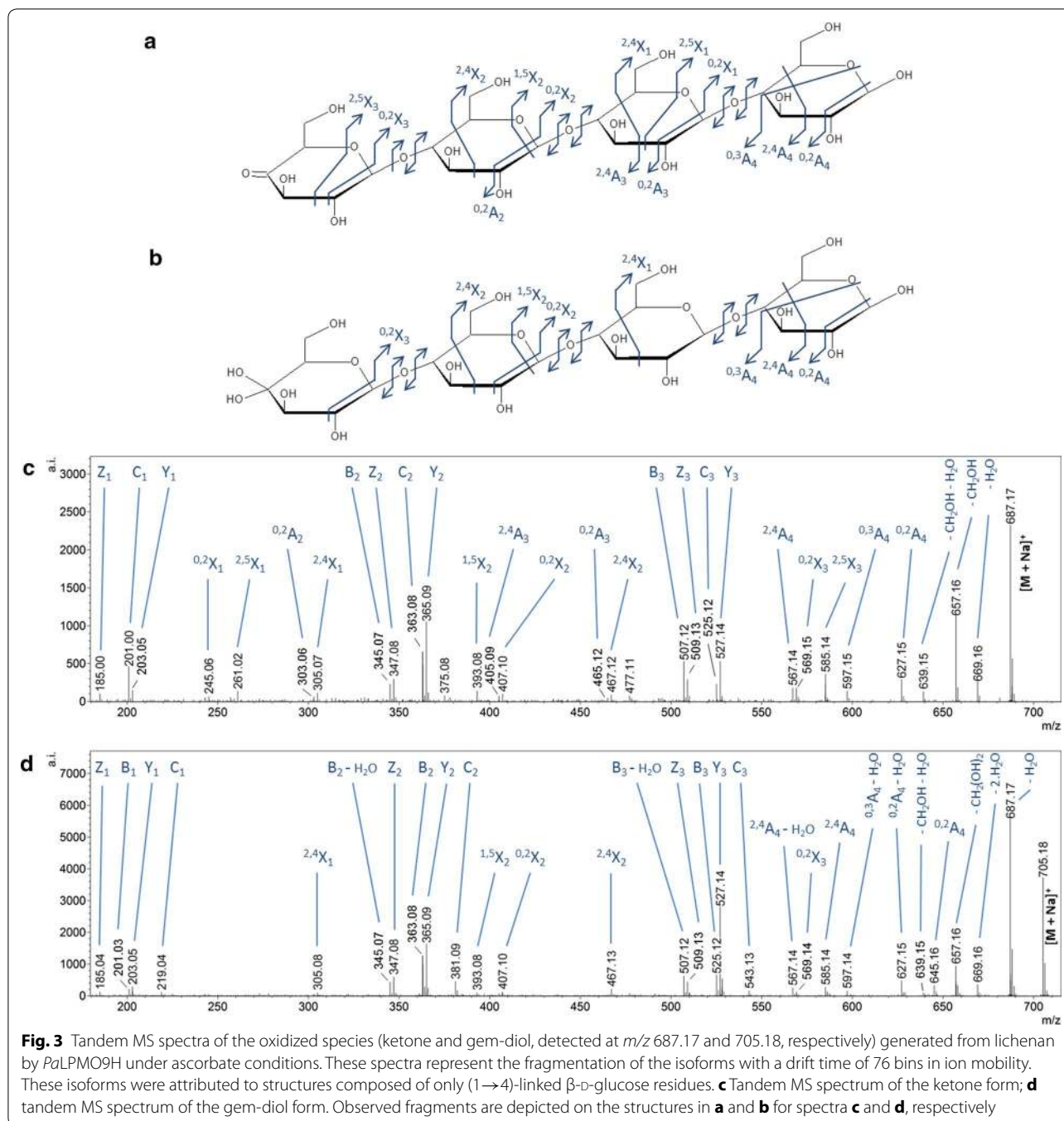
or three (DP4) adjacent  $\beta$ -(1  $\rightarrow$  4) linkages are predominant, while longer cellodextrin sequences contributed to less than 10% of the total polysaccharide chain in the starchy endosperm [23]. If one assumes that DP4 structures of different shapes have comparable ionization efficiency in MS, the peak area in Fig. 2 gives an estimate of the proportion of the two populations of DP4 differentiated by their ion mobility. The DP4 made of three consecutive  $\beta$ -(1  $\rightarrow$  4) bonds was released in high proportion following action of *PaLPMO9H* on MLG and lichenan substrates. DP5 species were also released from MLG and lichenan (Additional file 1: Figure S3). The most abundant peak ( $dt = 92$  bins) falls at the same drift time as the one measured from cellulose. Without excluding that those species arise in part from long cellodextrin stretches in the polymer, their abundance suggests that  $\beta$ -(1  $\rightarrow$  3) bonds linking consecutive cellotetraosyl units were cleaved by *PaLPMO9H*. Thus, in addition to  $\beta$ -(1  $\rightarrow$  4) linkages, *PaLPMO9H* appears able to catalyze the oxidative cleavage of  $\beta$ -(1  $\rightarrow$  3) linkages in  $\beta$ -(1  $\rightarrow$  4; 1  $\rightarrow$  3)-linked glucosidic substrates (MLG and lichenan).

The two DP4 oxidized degradation products ( $-2$  and  $+16$  Da compared to the non-modified form) from lichenan and MLG were further fragmented to confirm

their structures. In each case, ion mobility was used to distinguish between the isomers arising from  $\beta$ -(1  $\rightarrow$  4) and/or  $\beta$ -(1  $\rightarrow$  3) linkages. In accordance with the above discussion, the isoform displaying the lower drift time for each of these ions was attributed to a  $\beta$ -(1  $\rightarrow$  4)-linked oligosaccharide while the second isoform (higher drift time) presumably contained a mixture of  $\beta$ -(1  $\rightarrow$  3) and  $\beta$ -(1  $\rightarrow$  4) bonds. The corresponding tandem MS spectra are displayed in Fig. 3. Fragmentation of the ion at  $m/z$  687.17 ( $-2$  Da compared to the non-modified DP4, Fig. 3c) led to several fragments that are characteristic of a ketone form at the non-reducing end ( $^{2,5}X_1$ ,  $^{1,5}X_2$ ,  $^{2,5}X_3$ ). In contrast, the species at  $m/z$  705.18 ( $+16$  Da compared to the non-modified DP4, Fig. 3d) exhibited a double loss of water from the parent ion (indicated as  $-2$  H<sub>2</sub>O on the fragmentation spectrum) under fragmentation, which is a signature of an oxidized non-reducing end in the gem-diol form, as reported by Isaksen et al. [14]. The fragment  $^{1,5}X_2$ , observed at  $m/z$  393.08, further confirmed this structure. Since lichenan are linked through  $\beta$ -(1  $\rightarrow$  4) and/or  $\beta$ -(1  $\rightarrow$  3) bonds and taking into account the observations we have made previously, the oxidative cleavage by *PaLPMO9H* may have occurred on position C4 or C3. However, the fragmentation spectra for the two oxidized species ( $-2$  and  $+16$  Da) did not allow the determination of which position was oxidized among the C4 and C3 of the non-reducing end glycoside residue. Yet, for a simplified representation, the oxidation was positioned at C4 in the structures depicted in Fig. 3a, b. The second isoform separated by IM with a higher drift time was also fragmented for the two oxidized species. Similar to the first isoform, fragments indicating a ketone and a gem-diol on the non-reducing end were observed for the parent ions at  $m/z$  687.17 and  $m/z$  705.18, respectively (data not shown). Similar to the reaction products from lichenan, the two isoforms of the species at  $m/z$  687.19 produced from the MLG substrate were found to arise from a ketone at the non-reducing end, while both isoforms of the species at  $m/z$  705.18 were found to correspond to a gem-diol at the non-reducing end. In summary, *PaLPMO9H* oxidatively cleaved lichenan and MLG substrates, producing both ketone and gem-diols species at the non-reducing end glycoside residue. The exact positioning of the oxidation (C4 or C3) remained undetermined.

#### ***PaLPMO9H* is active toward $\beta$ -(1 $\rightarrow$ 4)-linked glucosidic substrates with branched sidechains**

To examine the mode of action of *PaLPMO9H* on xyloglucan, the tetradecasaccharide XXXGXXXG was used as a model substrate. Named according to the standard linear nomenclature, in which "G" represents an unbranched  $\beta$ -(1  $\rightarrow$  4)-linked glucosyl residue



and “X” represents  $\beta$ -(1 → 4)-linked Glc bearing an  $\alpha$ -(1 → 6)-linked xylosyl branch [24], XXXGXXXG presents a highly decorated backbone consisting of eight glucosyl residues. The MS spectrum of the products of cleavage of the XXXGXXXG preparation by *PaLP*MO9H (Fig. 1e) showed the presence of minor peaks, whose masses indicated the presence of sidechain galactosylation. They likely arose from a DP15 XyG,

which was present as minor impurity (roughly 5%) of the XXXGXXXG preparation as confirmed by both MS and HPAEC-PAD chromatogram of the substrate before incubation with *PaLP*MO9H (Additional file 1: Figure S4). In the latter structure (likely *XXLGXXXG* and/or *XXXGXXLG*), one of the laterally branched xylose bears a  $\beta$ -(1 → 2)-linked galactosyl (represented as “L” [24]).

Tandem MS analyses were performed on the species of  $m/z$  645.16, which uniquely matches a hydrated oxidized XX species (+16 Da from the non-modified oligosaccharide, Fig. 1e). The fragmentation spectrum suggested the coexistence of at least two oxidized species (Fig. 4). First, the double loss of water (indicated as  $-2\text{H}_2\text{O}$  on the fragmentation spectrum) from the precursor ion was found, which indicated a gem-diol at the non-reducing end. The  $^{0,1}\text{A}_2$  fragment was also observed. This fragment ion, corresponding to a loss of 46 Da from the parent, was reported by Isaksen et al. [14] as characteristic of an acidic function at the C1 of the reducing end.

These results clearly indicated that *Pa*LPMO9H was able to oxidatively cleave  $\beta$ -(1  $\rightarrow$  4)-linked glucose chains even in the presence of extensive lateral branching.

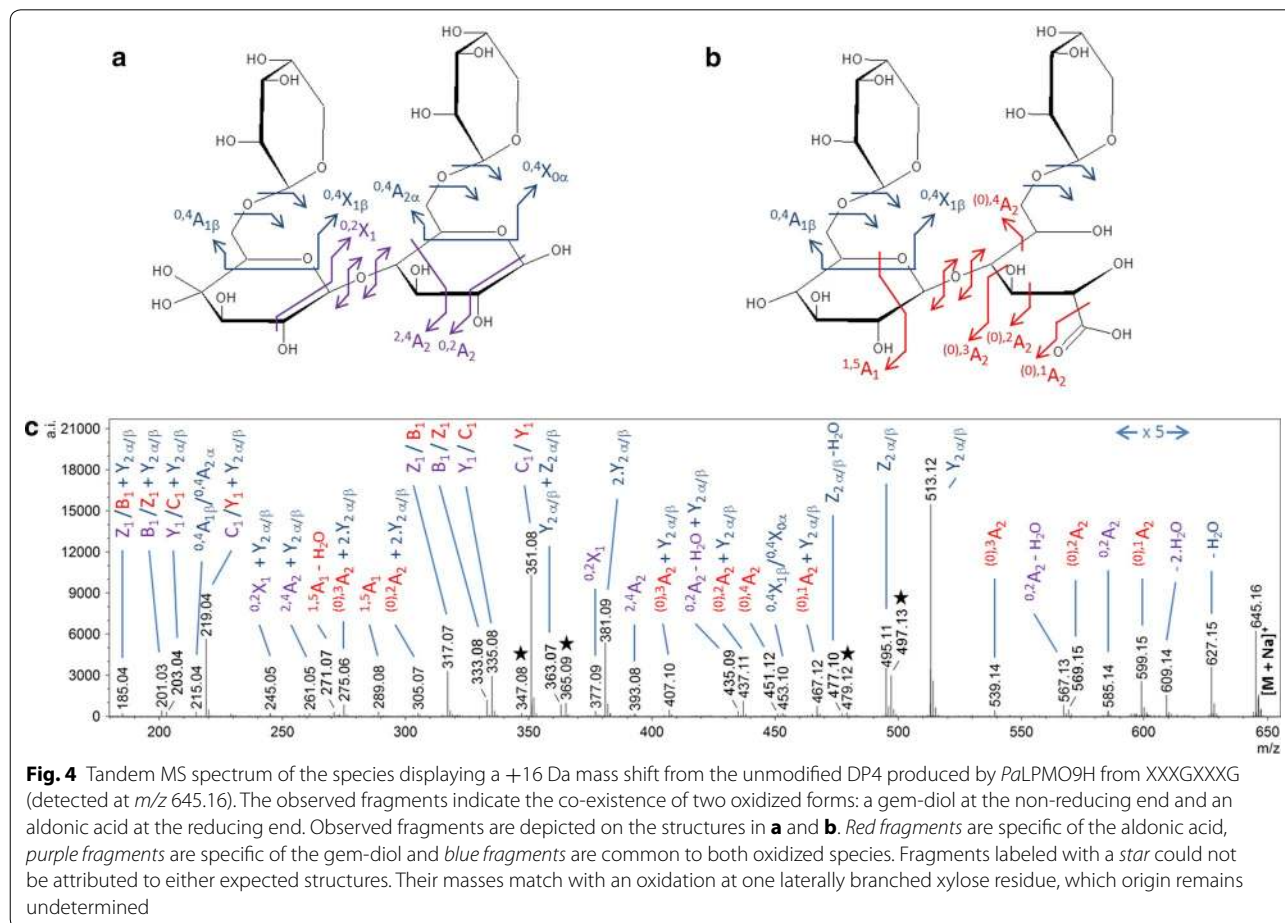
### Activity of *Pa*LPMO9H on $\beta$ -(1 $\rightarrow$ 4)-linked hetero-polysaccharides

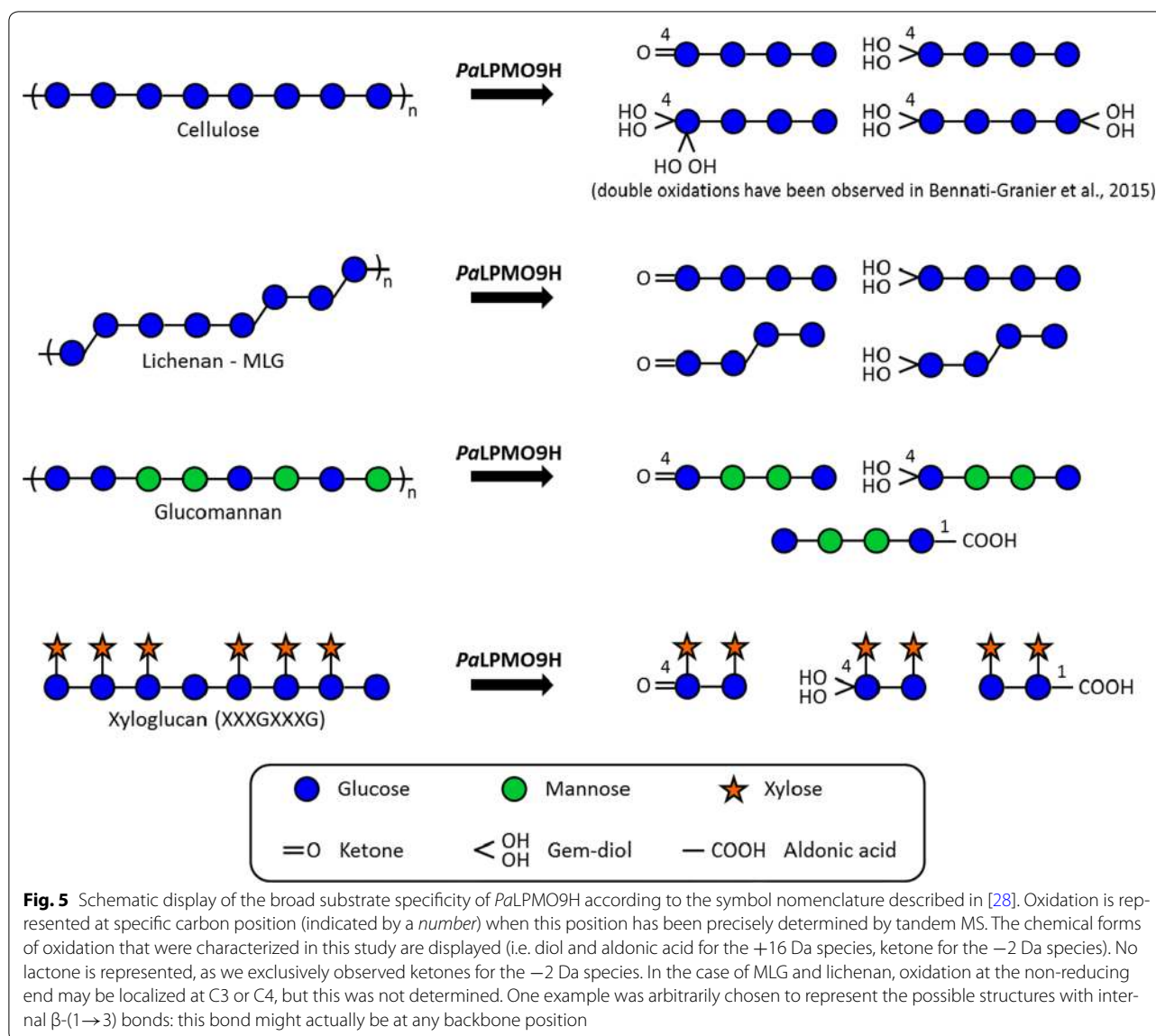
Glucomannans are mainly straight-chain polymers of  $\beta$ -(1  $\rightarrow$  4)-linked D-mannose and D-glucose. The product released at 705.18  $m/z$  corresponding to a +16 Da mass shift from the non-modified DP4 was fragmented

in tandem MS. The observed fragment ions showed the coexistence of two oxidized species with (i) the loss of 46 Da from the parent ion indicating a C1 oxidation (aldonic acid) at the reducing end, and (ii) a double loss of water from the precursor ion indicating a gem-diol at the non-reducing end (Additional file 1: Figure S5). On the other hand, fragmentation of the  $-2$  Da species showed unambiguously a single species, corresponding to a ketone form at the non-reducing end. It can thus be concluded that *Pa*LPMO9H oxidatively cleaved GM by forming oxidized species both at the reducing end and the non-reducing end. Since the main chain of GM consists of  $\beta$ -(1  $\rightarrow$  4)-linked residues, it can be presumed that the oxidized positions are at C1 and C4, respectively.

### Conclusion

A schematic representation compiling results of the present study is proposed in Fig. 5. Altogether, the results show that *Pa*LPMO9H is able to target polysaccharides differing from cellulose by their linkage types, glycosidic composition or the presence of sidechains. The broad substrate specificity of *Pa*LPMO9H could be





advantageous for *P. anserina*, which uses the most recalcitrant fraction of lignocellulose and therefore has to deal with highly variable polysaccharide structures. Recently, other fungal AA9 LPMOs have been shown to catalyze oxidative cleavage of cellulose and xyloglucan. They originate from the ascomycetes *Asperillus niger* (AN3046) [25] and *Fusarium graminearum* (*FgLPMO9A*) [26] and the brown-rot fungus *Gloeophyllum trabeum* (*GtLPMO9A-2*) [27]. Compared to these enzymes, *PaLPMO9H*

seems to behave differently. Although *FgLPMO9A* cleaves at both the C1 and C4 positions of cellulose and xyloglucan, it was not able to act on glucomannan or mixed-linkage  $\beta$ -glucans. Moreover, *NcLPMO9C* that displays similar substrate specificity to *PaLPMO9H* releases only C4-oxidized products. These subtle differences in terms of substrate specificity and regioselectivity within AA9 LPMOs could somewhat explain the multiplicity of AA9 genes in fungal saprotrophs.



## Additional file

**Additional file 1.** Structural characterization of products from incubation with the *Podospora anserina* lytic polysaccharide monoxygenase PaLPMO9H on beta-1,4-linked polysaccharides. **Figure S1.** Ion mobility recorded in negative ionization mode for the non-modified DP4 species ( $m/z$  665.2 Da) released from the incubation of PaLPMO9H with cellulose, MLG, Lichenan and for three commercial DP4. Drift times are indicated in bins (arbitrary units). Measurements were conducted in negative ion mode (i.e. on the  $[M-H]^-$  species) in order to make sure that none of the gas-phase isoform arose from different sites of cationization on the oligosaccharide. Thus, the drift times cannot be directly compared to those measured in Fig. 2, neither the relative proportion of the two main populations of DP4 differentiated by their ion mobility for MLG and Lichenan. **Figure S2.** Ion mobility recorded in positive ionization mode for the oxidized DP4 species released from the incubation of PaLPMO9H with cellulose, MLG, Lichenan. A: Ketone species ( $m/z$  687.2 Da) B: Gem-diol species ( $m/z$  705.2 Da). Drift times are indicated in bins (arbitrary units). **Figure S3.** Ion mobility recorded in positive ionization mode for the non-modified DP5 species ( $m/z$  851.2 Da) released from the incubation of PaLPMO9H with cellulose (black trace), MLG (green trace), Lichenan (red trace). Drift times are indicated in bins (arbitrary units). **Figure S4.** Analysis of the tetradecasaccharide XXXGXXXG substrate, prior incubation with the PaLPMO9H. A. ESI-MS spectrum showing the minor presence of XXLGXXXG or XXXGXXLG species. B. High-performance anion-exchange chromatogram indicating the presence of minor peaks likely corresponding to XXLGXXXG and XXXGXXLG. Peak integration reveals that they represent ca. 5% of the total oligosaccharide content. **Figure S5.** Tandem MS spectrum of the species displaying a +16 Da mass shift from the unmodified DP4 produced by PaLPMO9H from GM (detected at  $m/z$  705.2). The observed fragments indicate the co-existence of two oxidized forms: A gem-diol at the non-reducing end and an aldonic acid at the reducing end. Observed fragments are depicted on the structures in panels A and B. Red fragments are specific to the aldonic acid, purple fragments are specific to the gem-diol and blue fragments are common to both oxidized species.

### Abbreviations

AA: auxiliary activity enzyme; PaLPMO9: *Podospora anserina* AA9 LPMO; LPMO: lytic polysaccharide monoxygenase; MLG: barley mixed-linkage  $\beta$ -glucan; XyG: tamarind xyloglucan; GM: konjac glucomannan; DP: degree of polymerization.

### Authors' contributions

HR and JGB designed the research. MF, NM and SG performed the research experiments. MF, SG, DR, NM, HB, HR and JGB analyzed the data. MF, HR and JGB drafted the manuscript. All authors read and approved the final manuscript.

### Author details

<sup>1</sup> Unité de Recherche Biopolymères, Interactions, Assemblages, INRA, 44316 Nantes, France. <sup>2</sup> Polytech Marseille, UMR1163 Biodiversité et Biotechnologie Fongiques, INRA, Aix-Marseille Université, Avenue de Luminy, 13288 Marseille, France. <sup>3</sup> Michael Smith Laboratories, University of British Columbia, 2185 East Mall, Vancouver, BC V6T 1Z4, Canada. <sup>4</sup> Department of Chemistry, University of British Columbia, 2036 Main Mall, Vancouver, BC V6T 1Z1, Canada. <sup>5</sup> Department of Biochemistry, University of British Columbia, 2350 Health Sciences Mall, Vancouver, BC V6T 1Z3, Canada. <sup>6</sup> Department of Botany, University of British Columbia, 6270 University Boulevard, Vancouver, BC V6T 1Z4, Canada.

### Acknowledgements

The authors would like to thank M. Haon and S. Grisel for technical assistance. N.M. thanks the Natural Sciences and Engineering Research Council of Canada (NSERC) for an Alexander Graham Bell Canada Graduate Doctoral Scholarship.

### Competing interests

The authors declare that they have no competing interests.

### Availability of supporting data

All data generated or analyzed during this study are included in this published article and its Additional files.

### Consent for publication

All authors approved the final version of the manuscript.

### Funding

This study was funded by the AMIDEX foundation (Funcopper project, Grant Number A\*M-AAP-EI-13-13-130115-15.37 and MicrobioE project, Grant Number ANR-11-IDEX-0001-02). Work in Vancouver was additionally supported by NSERC (Discovery Grant), the Canada Foundation for Innovation and the British Columbia Knowledge Development Fund.

Received: 2 November 2016 Accepted: 2 March 2017

Published online: 11 March 2017

### References

- Gupta VK, et al. Fungal enzymes for bio-products from sustainable and waste biomass. *Trends Biochem Sci.* 2016;41(7):633–45.
- Sigoillot J-C, et al. Fungal strategies for lignin degradation. In: Jouann L, Lapierre C, editors. *Lignins: biosynthesis, biodegradation and bioengineering.* Cambridge: Academic Press; 2012. p. 263–308.
- Vaaje-Kolstad G, et al. An oxidative enzyme boosting the enzymatic conversion of recalcitrant polysaccharides. *Science.* 2010;330(6001):219–22.
- Beeson WT, et al. Oxidative cleavage of cellulose by fungal copper-dependent polysaccharide monoxygenases. *J Am Chem Soc.* 2012;134(2):890–2.
- Quinlan RJ, et al. Insights into the oxidative degradation of cellulose by a copper metalloenzyme that exploits biomass components. *Proc Natl Acad Sci USA.* 2011;108(37):15079–84.
- Harris PV, et al. Stimulation of lignocellulosic biomass hydrolysis by proteins of glycoside hydrolase family 61: structure and function of a large, enigmatic family. *Biochemistry.* 2010;49(15):3305–16.
- Johansen KS. Discovery and industrial applications of lytic polysaccharide mono-oxygenases. *Biochem Soc Trans.* 2016;44:143–9.
- Levasseur A, et al. Expansion of the enzymatic repertoire of the CAZy database to integrate auxiliary redox enzymes. *Biotechnol Biofuels.* 2016;6:14.
- Walton PH, Davies GJ. On the catalytic mechanisms of lytic polysaccharide monoxygenases. *Curr Opin Chem Biol.* 2016;31:195–207.
- Hemsworth GR, et al. Discovery and characterization of a new family of lytic polysaccharide monoxygenases. *Nat Chem Biol.* 2014;10(2):122–6.
- Lo Leggio L, et al. Structure and boosting activity of a starch-degrading lytic polysaccharide monoxygenase. *Nat Commun.* 2015;6:9.
- Forsberg Z, et al. Comparative study of two chitin-active and two cellulose-active AA10-type lytic polysaccharide monoxygenases. *Biochemistry.* 2014;53(10):1647–56.
- Agger JW, et al. Discovery of LPMO activity on hemicelluloses shows the importance of oxidative processes in plant cell wall degradation. *Proc Natl Acad Sci USA.* 2014;111(17):6287–92.
- Isaksen T, et al. A C4-oxidizing lytic polysaccharide monoxygenase cleaving both cellulose and cello-oligosaccharides. *J Biol Chem.* 2014;289(5):2632–42.
- Bennati-Granier C, et al. Substrate specificity and regioselectivity of fungal AA9 lytic polysaccharide monoxygenases secreted by *Podospora anserina*. *Biotechnol Biofuels.* 2015;8:14.
- Frandsen KEH, et al. The molecular basis of polysaccharide cleavage by lytic polysaccharide monoxygenases. *Nat Chem Biol.* 2016;12(4):298.
- Frommhagen M, et al. Discovery of the combined oxidative cleavage of plant xylan and cellulose by a new fungal polysaccharide monoxygenase. *Biotechnol Biofuels.* 2015;8:12.
- Espagne E, et al. The genome sequence of the model ascomycete fungus *Podospora anserina*. *Genome Biol.* 2008;9(5):22.
- Couturier M, et al. Plant biomass degrading ability of the coprophilic ascomycete fungus *Podospora anserina*. *Biotechnol Adv.* 2016;34(5):976–83.

20. Bey M, et al. Cello-oligosaccharide oxidation reveals differences between two lytic polysaccharide monoxygenases (Family GH61) from *Podospora anserina*. *Appl Environ Microbiol*. 2013;79(2):488–96.
21. Scheller HV, Ulvskov P. Hemicelluloses. In: Merchant S, Briggs WR, Ort D, editors. Annual review of plant biology. Santa Clara: Palo Alto; 2010. p. 263–89.
22. McGregor N, et al. Structure-function analysis of a mixed-linkage beta-glucanase/xyloglucanase from the key ruminal bacteroidetes *Prevotella bryantii* B(1)4. *J Biol Chem*. 2016;291(3):1175–97.
23. Burton RA, Fincher GB. Current challenges in cell wall biology in the cereals and grasses. *Front Plant Sci*. 2012;3:6.
24. Tuomivaara ST, et al. Generation and structural validation of a library of diverse xyloglucan-derived oligosaccharides, including an update on xyloglucan nomenclature. *Carbohydr Res*. 2015;402:56–66.
25. Jagadeeswaran G, et al. A family of AA9 lytic polysaccharide monoxygenases in *Aspergillus nidulans* is differentially regulated by multiple substrates and at least one is active on cellulose and xyloglucan. *Appl Microbiol Biotechnol*. 2016;100(10):4535–47.
26. Nekiunaite L, et al. FgLPMO9A from *Fusarium graminearum* cleaves xyloglucan independently of the backbone substitution pattern. *FEBS Lett*. 2016;590(19):3346–56.
27. Kojima Y, et al. A lytic polysaccharide monoxygenase with broad xyloglucan specificity from the brown-rot fungus *Gloeophyllum trabeum* and its action on cellulose-xyloglucan complexes. *Appl Environ Microbiol*. 2016;82(22):6557–72.
28. Varki A, et al. Symbol nomenclature for glycan representation. *Proteomics*. 2009;9(24):5398–9.

Submit your next manuscript to BioMed Central and we will help you at every step:

- We accept pre-submission inquiries
- Our selector tool helps you to find the most relevant journal
- We provide round the clock customer support
- Convenient online submission
- Thorough peer review
- Inclusion in PubMed and all major indexing services
- Maximum visibility for your research

Submit your manuscript at  
[www.biomedcentral.com/submit](http://www.biomedcentral.com/submit)

